

# Wind Cooling Effect on Dynamic Overhead Line Ratings

J Fu  
[jfu03@qub.ac.uk](mailto:jfu03@qub.ac.uk)

S Abbott  
[sabbott01@qub.ac.uk](mailto:sabbott01@qub.ac.uk)

B Fox  
[b.fox@ee.qub.ac.uk](mailto:b.fox@ee.qub.ac.uk)

D J Morrow  
[dj.morrow@ee.qub.ac.uk](mailto:dj.morrow@ee.qub.ac.uk)

S Abdelkader  
[s.abdelkader@qub.ac.uk](mailto:s.abdelkader@qub.ac.uk)

Queen's University Belfast, UK

**Abstract** – Due to deregulation of the power supply industry and the continuing need for network expansion, there is pressure to maximise utilisation of the existing transmission and distribution networks. A way of achieving this is to employ dynamic line ratings instead of the present static line ratings based on conservative weather assumptions. Such an approach is especially beneficial in areas of significant wind generation. In dynamic line rating methodologies, both the line loading and weather conditions are major contributors to a conductor's temperature. The effects of Joule heating and wind speed have been examined using a section of 'Lynx' 175 mm<sup>2</sup> conductor in a wind tunnel under controlled environmental conditions.

**Index Terms**--Dynamic line rating, wind cooling effect

## I. INTRODUCTION

Traditional overhead line ratings are determined based on seasonal weather conditions to provide both essential clearances for safety and long lifetime of the conductors. Most utilities set line ratings statically. For example, the UK Energy Association's Engineering Recommendation P27 [1] provides ratings based on assumed average ambient temperatures of 2 °C, 9 °C and 20 °C in winter, spring/autumn and summer respectively. Besides, an average wind speed of 0.5 m/s is assumed, and the effect of solar radiation on the line is not taken into account in P27.

In most circumstances, the static line ratings are likely to underestimate the actual ampacity of the line, as they are too conservative, especially under high wind conditions. Therefore, the extra capacity of the dynamic relative to the static line ratings provides an economic solution to improve the utilisation of the existing transmission and distribution networks. The dynamic line rating (DLR) estimates the line ampacity in real time with instant monitored weather conditions, taking account of the wind cooling effect. In particular, high wind speeds provide extra line cooling and ampacity, when the additional capacity is needed to accommodate higher wind generation.

In Northern Ireland (NI) and the Republic of Ireland (RoI), an increased amount of renewable generation is being connected to the network due to a target of 42% from renewable generation by 2020, mainly from wind power [2]. Renewable penetration currently stands at about one third of the target, and the rate of growth is such that there is every chance that the target may be met. The relation between DLR

and wind generation has the potential to allow significant future wind power feed-in with minimal reinforcement in network capacity, especially at sub-transmission level – 110 kV in NI. Even when the dynamic estimate of ampacity is less than the static line rating, the approach can ensure that the conductors are effectively protected from thermal violation.

Line-rating methodologies such as those outlined in CIGRE [3] and IEEE [4] state that both the line loading and weather conditions are major contributors to a conductor's temperature. The steady-state thermal behaviour is determined by the balance between heat gains and heat losses of the conductor, as expressed in Eqn. 1.

$$P_J + P_M + P_S + P_i = P_c + P_r + P_w \quad (1)$$

In Eqn. 1,  $P_J$  is Joule heating,  $P_M$  is magnetic heating,  $P_S$  is solar heating and  $P_i$  is corona heating, while  $P_c$  is convective cooling,  $P_r$  is radiative cooling and  $P_w$  is evaporative cooling.

In this heat balance equation, Joule heating and (forced) convection cooling are the crucial components for DLR. Hence the focus of the experimental work presented here has been on the effect of wind speed on the temperature of a conductor carrying current. The experiments consisted of a still air test and forced convection tests.

## II. EXPERIMENTAL PROGRAMME

The experimental programme was designed to complement field testing of two 110 kV lines in the Northern Ireland Electricity (NIE) network [5]. It was found that it was difficult to assess the individual dependencies of conductor temperature on wind, wind direction, ambient temperature and solar radiation, all of which were subject to the vagaries of the Northern Irish weather.

In order to assess each individual factor in the DLR methodology, two test rigs were constructed. The rigs were used to examine the thermal behaviour of the conductor under controlled environmental conditions with and without the forced convection. It was assumed that the solar heating was negligible, as both testing facilities were located away from direct sunlight. The aluminum conductor steel reinforced

(ACSR) ‘Lynx’ 175 mm<sup>2</sup> conductors, with a maximum allowed temperature of 75 °C, were used in the tests, as it is used in the selected 110 kV circuits that are the subject of the field testing [5]. These circuits were chosen as they will bear the brunt of planned wind generation, and are expected to provide an early indication of the feasibility of DLR for future wind farm connections. Moreover, the fully greased ACSR are the most common conductors used in the NIE network, on account of their resistance to corrosion in a maritime climate. The electrical properties of this type of conductor are indicated in Table I.

TABLE I  
PROPERTIES OF LYNX 175 MM<sup>2</sup> CONDUCTOR

Code Name: Lynx		Nominal Al Area: 175 mm <sup>2</sup>				
Stranding and Wire Diameter (mm)		Cross Sectional Area (mm <sup>2</sup> )			Overall Diameter (mm)	Calculated DC Resistance at 20 °C (Ω/km)
Al	Steel	Al	Steel	Total		
30/2.79	7/2.79	183.4	42.80	226.2	19.53	0.1567

#### A. Still air test rig

As shown in Fig. 1, a section of conductor was strung using plastic brackets which were attached to the walls to reduce the conductor’s heat dissipation through the walls. The conductor was energized by a step-down voltage transformer with a turns ratio of 128:1, and the primary side was connected to a variable transformer supplied at 230 V and 50 Hz. The transformer could provide a continuous current up to 653 A through 3 feed cables to the conductor, and the current flow could be controlled by adjusting the variable transformer. A clamp meter was used for current measurements.

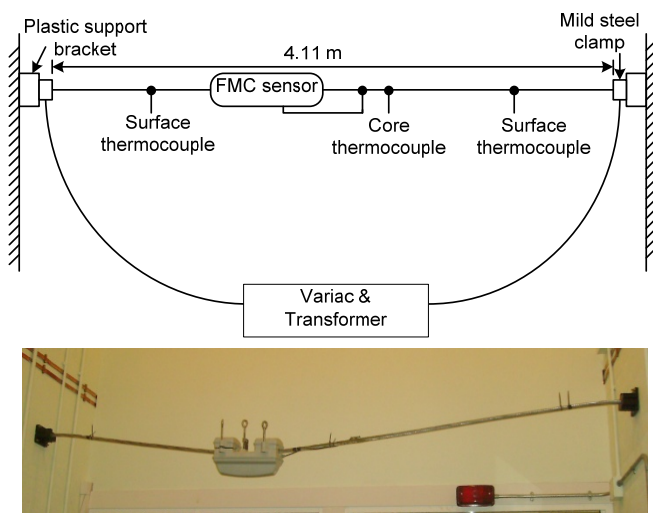


Fig. 1 Still air test rig

The positions of the calibrated standard k-type thermocouples are indicated in the schematic. Two

thermocouples were attached on the conductor’s surface using a heat sink compound to ensure good heat transfer, and wrapped in a single layer of Denso tape. Another thermocouple was located at the centre of the conductor through a 3 mm hole drilled into the conductor, as shown in Fig. 2, for core temperature measurement. The FMC real-time monitoring equipment, used in the field test, was also mounted on the circuit for calibration purposes.

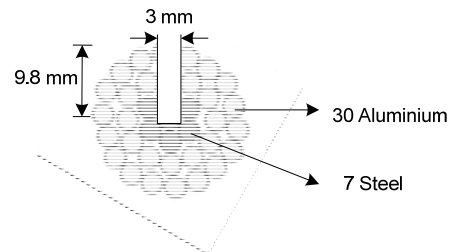


Fig. 2 Conductor core temperature measurement

#### B. Wind tunnel test rig

In the wind tunnel test rig, laminar wind with controlled speed could be provided perpendicular to the conductor’s axis, as shown in Fig. 3. The conductor in the wind tunnel was cut to 1.5 m due to the confined space, while the other facilities remain the same as for the still-air test. Three thermocouples were attached to the conductor, of which two were surface mounted windward and leeward, and one was inserted in the core. A calibrated FC0510 micromanometer was used to measure the wind speeds.



Fig. 3 External and internal view of wind tunnel test rig

### III. EXPERIMENTAL DATA ANALYSIS

#### A. Joule Heating Effect

##### 1) Stepped current tests

Fig. 4 demonstrates the changes of conductor surface temperature in a period of 60 minutes when subjected to two different stepped currents: one from 0 A to 250 A, and the other from 0 A to 500 A. In order to maintain the constant currents, the variable transformer was adjusted during the tests. The initial conductor temperatures in both tests were 18.4 °C, the ambient room temperature. From the graphs, both characteristics show that the conductor temperature increase takes the form of a standard first-order temperature rise and appears to converge towards a final temperature when the conductor has reached a steady-state operating point. In the steady-state condition, the conductor temperature is established by a balance of heat generated by ohmic losses with heat radiated and heat removed by the surrounding air through natural convection. Apparently, the higher current would produce a much greater final temperature.

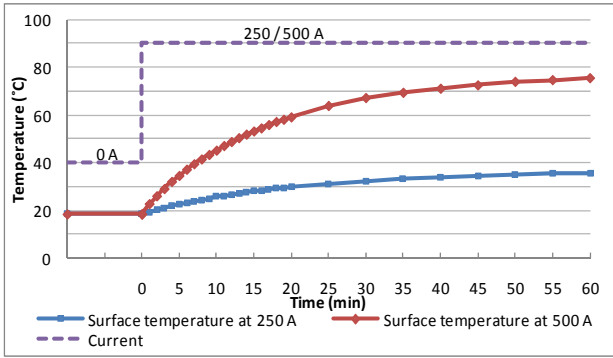


Fig. 4 Response of conductor surface temperature to current steps

##### 2) Conductor surface and core temperature comparisons

Utilities usually monitor overhead line surface temperature in the DLR application rather than core temperature due to easy assembly and conductor protection. In fact, the conductor mid-span sag depends on core temperature, which is not the same as surface temperature. It may be observed from Fig. 5 that the core and surface temperatures behave slightly differently. The core temperature initially increases slightly slower than that of the surface, but exceeds the surface temperature after about 14 minutes, and indeed reaches a higher final temperature than that of the surface. The core temperature exceeds the surface temperature by 6.1% (4.6 °C) at the end of the 60-minute period. As most of the current is passing through the aluminum strands, the substantial heat generated due to ohmic losses in the aluminum leads to the greater initial rate of increase in conductor surface temperature compared to the steel core. However, the increasing temperature difference between the conductor surface and ambient air gradually enhances the natural convection from the aluminum. By contrast, the heat generated by the steel core can only be dissipated to the surrounding aluminum strands with a much smaller

temperature difference. Therefore, it is harder for the core to dissipate its heat, resulting in a greater final temperature in the core than on the surface. In practical ampacity prediction, measured surface temperature is widely used, so a reasonable margin is required to ensure minimum ground clearance.

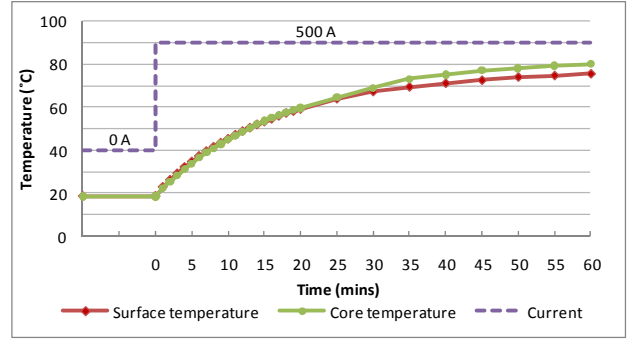


Fig. 5 Surface and core temperature test (0 to 500 A)

##### 3) Current behaviour in dynamic thermal exchanges

While the conductor was heated by ohmic losses, the a.c. resistance, which depends on frequency, average current density and temperature, increased. As suggested in [3], the a.c. resistance per unit length can be calculated as follows:

$$R_{ac} = k_j R_{dc} [1 + \alpha(T_{av} - 20)] \quad (2)$$

$R_{dc}$  is the d.c. resistance at 20 °C per unit length,  $\alpha$  is the temperature coefficient of resistance per degree Kelvin,  $T_{av}$  is the mean temperature of the conductor, and  $k_j$  is a constant that takes into account the increase in resistance due to skin effect, with a suggested value of 1.0123 [6].

According to Eqn. 2, the a.c. resistance is taken to depend only on conductor temperature, as the other variables are considered to be constant. Consequently, if the variable transformer were not adjusted, an exponential decay in current with an initial value of 550 A would be expected during the thermal transient, as shown Fig. 6, tending towards a steady-state value under thermal equilibrium. The fluctuations around the exponential decay of current in Fig. 6 are probably due to minor supply voltage variations.

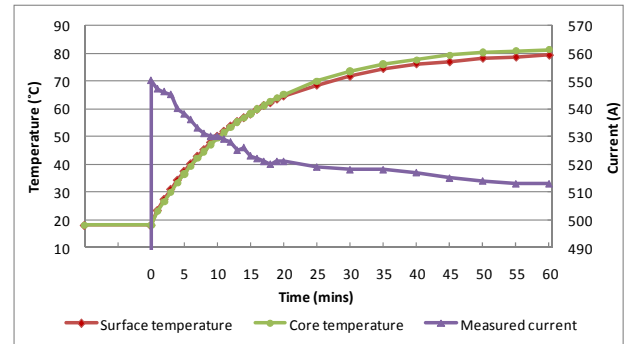


Fig. 6 Current behaviour with changes of conductor temperature

## B. Wind Cooling Effect

### 1) Effect of wind speed on conductor cooling

The conductor temperature was monitored in the wind tunnel with forced convection at various wind speeds. A step change in current from 0 to 550 A was applied as shown in Fig. 7. The initial ambient temperature in each test was within  $23.1 \pm 1.3$  °C. The selected wind speeds were 0, 1, 3, 5, 10 and 15 m/s with a wind attack angle of  $90^\circ$ , i.e. normal to the conductor axis. The results shown in Fig. 7 are for the core temperature. It should be noted that the current was not adjusted to be constant during the tests, so that the Joule heating from the conductor would be slightly less than that for the constant current condition. An experimental result shows that the steady-state temperature difference with and without adjusting current was 6 °C with an initial current of 500 A in still air conditions, and the disparity decreases with increasing wind speed. The final steady-state current in each case was in the range 513 - 525 A.

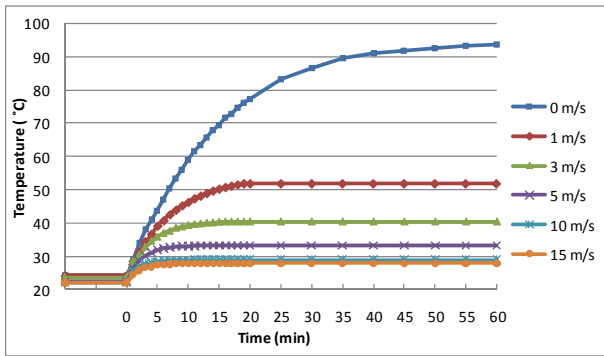


Fig. 7 Wind cooling of conductor for various wind speeds (0 – 550 A)

When the conductor was subjected to forced convection in the wind tunnel, the heat dissipation was due mainly to forced convection and radiation. It was observed that the higher the wind speed, the lower the final conductor temperature. A decrease of 44.6% is achieved when the wind speed was increased from 0 to 1 m/s, which provides a dramatic cooling effect on conductor temperature, and hence more current can be carried. With increasing wind speed, the wind cooling effect on conductor temperature becomes less significant. For a typical cut-in speed of wind turbine, which is 4 m/s, the large potential is provided to accommodate extra wind generation while the cooling effect by wind is significant.

Fig. 7 also shows that the transient time to reach the steady-state conductor temperature is effectively shortened when the higher wind speed is applied. The corresponding thermal time constants to obtain 63.2% of a change from the initial temperature to the final temperature are represented in Fig. 8. The observed time constant is reduced exponentially, and tends to converge when there is a linear increase in wind speed. Therefore, the thermal time constant at any specific wind speed can be predicted using the characteristic at the same atmospheric conditions, which is an important factor in estimating emergency ratings. Furthermore, in DLR

application, if a steady-state physical model, such as the CIGRE or IEEE methodology, is employed to predict the conductor temperature, the prediction will be less accurate in low wind speed condition due to the longer delay in the thermal transient process.

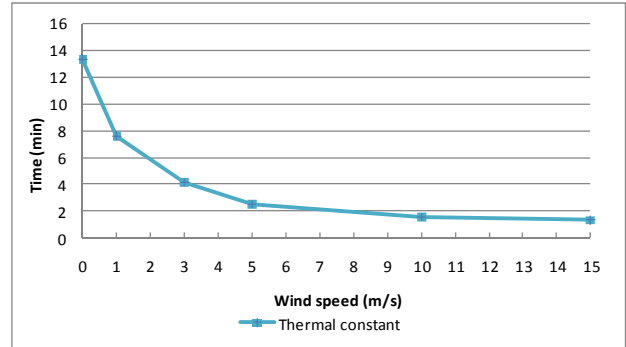


Fig. 8 Thermal time constants at various wind speeds

### 2) Comparisons of windward and leeward sides of conductor

Fig. 9 shows the core, leeward and windward temperatures of the conductor in the steady state under different wind conditions. The overall trend in the temperatures is consistent with the observation that the improvement in conductor cooling is much more significant at lower wind speeds, while the decrease in equilibrium temperature becomes negligible as the wind speed is increased from 5 m/s to 15 m/s.

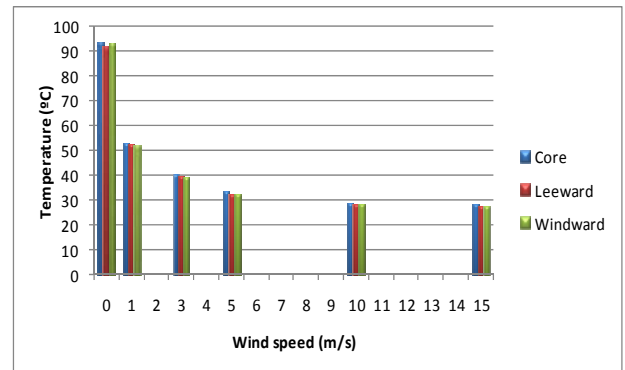


Fig. 9 Steady-state conductor temperatures at different wind speeds

Although the temperature differences in the core, leeward surface and windward surface are less visible in the figure compared to the overall changes, the relationship in conductor temperature at these different locations is also related to wind speed. The detailed variations in temperature differences between surface and core temperatures at various wind speeds are shown in Fig. 10. The temperature difference between the leeward side and the core is represented by the dashed line, while the difference for the windward side is shown as a solid line. From a number of still air tests, it was observed that the conductor's temperatures were not evenly

distributed along the surface due to the stranded configuration, conductor materials and hot spots from damaged strands, etc. At a wind speed of 0 m/s, i.e. the still air condition, the surface temperature on both sides of the conductor are below the core temperature in the steady state, and the leeward surface temperature is 0.9 °C lower than the windward surface temperature, so that the sensor position on the windward side normally indicates a higher temperature compared to leeward without forced convection. With the increase of wind speed, the windward side is exposed to the wind source, resulting in a lower temperature than on the leeward side. The temperature differences between the two sides in the equilibrium state were effectively reduced with increasing wind speed, being 0.6, 0.5, 0.2, and 0 °C at speeds of 1, 3, 5 and 10 m/s respectively. Besides, at the beginning of the transient state, the tendency of the conductor surface to heat up faster than the core, due to the greater current flowing through the outer aluminium strands, is weakened by increased wind speeds. For example, the core temperature was never exceeded throughout the test at a wind speed of 5 m/s or greater, because the forced convection accelerated the heat dissipation from the conductor surface. Comparing the surface temperature of both sides, it takes longer to be cooled below core temperature at the leeward side as less wind is experienced than windward. In conclusion, higher wind speed will be helpful in distributing heat evenly along a conductor's surface, and will reduce the incidence of hot spots.

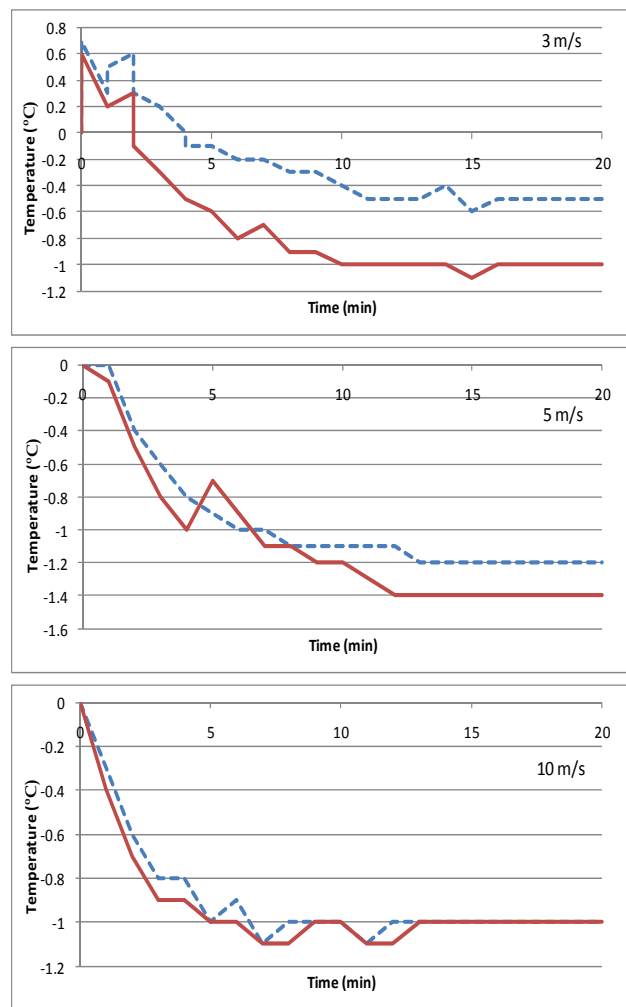
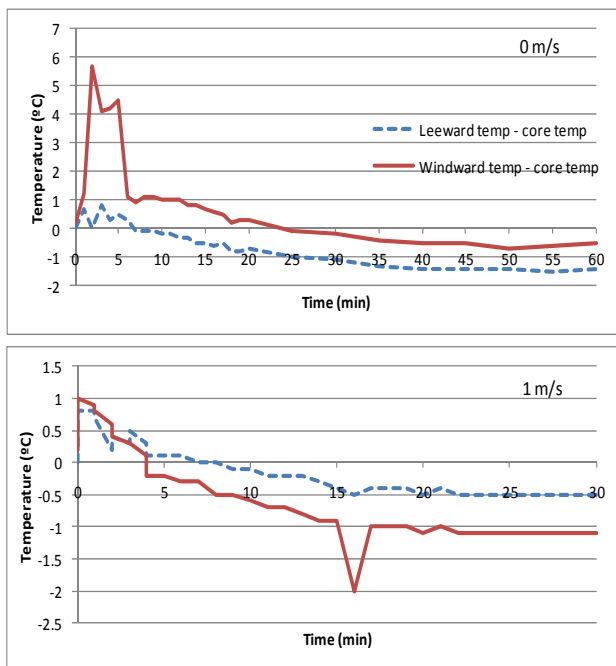


Fig. 10 Temperatures of windward/leeward surfaces relative to the core at various wind speeds

#### IV. CONCLUSION

These experiments have provided practical data to enable the individual factors related to dynamic line rating to be quantified. They highlight the role that wind plays in line cooling and would suggest that, in most circumstances, the dynamic line rating is greater and more accurate than the static line rating, as static ratings assume a wind speed of 0.5 m/s. The experiments in a wind tunnel were conducted in an ideal wind condition with laminar air and without gusts due to a number of filters. In reality, the uncertainty of wind speed, direction and turbulence are topography dependent, and a real-time monitoring system will provide actual atmospheric conditions for ampacity prediction at a given time and place.

As wind farms have a cut-in speed around 4 m/s, the network will be able to accommodate more power due to the cooling effect provided by forced convections. However, the monitored site may be distant from any wind farms and experience different weather conditions, so that transferred power would be limited by those sections of the network with the least cooling. For these sheltered sections, the ampacity

could be improved by restringing with new conductor which has higher maximum allowed temperature.

The application of DLR will effectively increase the line ampacity with low cost, and thus negate or postpone the necessity to upgrade the existing network to accommodate greater renewable energy generation.

## V. FUTURE WORK

Further to the wind cooling effect tests, ampacity tests will also be implemented with the conductor remaining at its maximum allowed temperature at various wind speeds. These experiments will quantify the improvement in a conductor's ampacity with controlled forced convection, and investigate the effectiveness of DLR.

It should be noted that protection systems in existing transmission and distribution grids will need to be updated to accommodate the dynamic line rating. It is envisaged that it will be necessary to implement adaptive over-current protection to take account of the changing ampacity of lines where DLR is applied.

It will also be necessary to assess the impact of increased line ratings on the electrical behaviour of lines. For example, availing of increased ampacity will result in increased losses. It may be decided to upgrade a line on economic grounds to reduce losses, even though it can provide the necessary dynamic rating.

Another factor that may limit line loading within the dynamic line rating is voltage regulation. Typically, transmission and sub-transmission voltages should be held within 6% of the nominal rating. A point will be reached where the length of a circuit is such that voltage regulation limits transmissible power rather than the dynamic thermal rating.

Proper evaluation of all the issues that affect the capability of a network in a wind power exporting region can only be assessed through study of a wide range of possible operating scenarios. It will be necessary to ensure a satisfactory voltage profile and dynamic stability within the operating envelope defined by dynamic line ratings. Ultimately, network planning will be governed by the balance between the economic loss due to wind power curtailment on the one hand, and the cost of reinforcement on the other.

## ACKNOWLEDGEMENTS

The authors wish to acknowledge financial support provided by Science Foundation Ireland under the Strategy for Science, Technology and Innovation (2006-2013). The authors also wish to thank the many experts who have contributed specialised knowledge to the project, and the other project partners, NIE, RES, Airtricity and FMC Technology, for their support.

## REFERENCES

- [1] Energy Network Association. "Engineering Recommendation P27: current rating guide for high voltage overhead lines operating in the UK distribution system". 1986
- [2] DETI (NI) and DCENR (RoI). "All-island Grid Study". 2008
- [3] CIGRE Working Group 22.12. "Thermal behaviour of overhead conductors". CIGRE 207, 2002
- [4] IEEE T&D Committee. "Calculating the current-temperature of bare overhead conductors". IEEE Standard 738, 2006.
- [5] Abdelkader, S, Abbott, S, Fu, J, Fox, B, Flynn, D, McClean, L and Bryans, L. "Dynamic monitoring of overhead line ratings in wind intensive areas". EWEC 2009, Marseille, 2009
- [6] Price, C F and Gibbon, R P. "Statistical approach to thermal rating of overhead lines for power transmission and distribution". IEE Proceedings, Vol. 130C, 1983, pp. 245-256

## BIOGRAPHIES



**Jiao Fu** received a 1<sup>st</sup> class B.Eng. degree in Electrical and Electronic Engineering in 2009 from Queen's University Belfast, U.K., where she is currently working toward the Ph.D. degree on dynamic overhead line rating, and wind power integration into electrical grids.



**Stephen Abbott** received a 1<sup>st</sup> class M.Eng. degree from Queen's University Belfast (QUB) in 2009. He is currently pursuing a Ph.D. at QUB. His research interests include distributed generation, reactive power and dynamic line rating.



**Brendan Fox** received the B.Sc. and Ph.D. degrees from Queen's University Belfast (QUB) in 1966 and 1969. Following a period with the Central Electricity Generating Board in Great Britain, he joined the Ulster Polytechnic as a Lecturer in 1972. He was then appointed to a lectureship at QUB in 1980, where he is now Emeritus Professor of Power Systems Engineering. His main research interest is in the integration of wind power on a significant scale. Professor Fox is a member of the IET.



**D. John Morrow** was born in Dungannon, Northern Ireland, in 1959. He received the B.Sc and Ph.D. degrees from Queen's University Belfast (QUB), U.K., in 1982 and 1987, respectively. He is now a Reader in electrical engineering at QUB, where he has been since 1987, with research and consulting interests in electric power systems, power system instrumentation, and gen-set controllers. Dr. Morrow is a member of the IET and also a member of the IEEE PES Excitation Systems Subcommittee.



**Sobhy M. Abdelkader** was born in Salahat, Egypt in 1961. He obtained the B. Sc., M.Sc. and Ph.D. degrees all in Electrical Engineering from Mansoura University, Egypt in 1984, 1989 and 1995 respectively. Since 1984, he has been employed by the Electrical Engineering Department at Mansoura University, where he is now a professor. He joined Queen's University Belfast as a Senior Research Fellow in Nov. 2007. His research interests include power system analysis and control, wind power integration into electrical grids, and electrical energy markets.